D．考察

1. 本年度に名古屋大学により実施された心筋細胞組織の磁気測定では、生体の電流は数μA オーダーと考えられるため、SQUID を使用した場合を考えると、感磁部と組織の距離（数 10mm）から約数 10pT 程度の生体磁界を検出する。これに対して、微細コイルを用いた本センサでは 1mm 以内に感磁部を設置することができる。磁界強度は距離に比例するため、被測定磁界の大きさは数 10 倍(数 100pT オーダー)となり、本センサでは磁界検出が大幅に有利となる。

2. 比透磁率10000のワイヤであれば磁界40～50μTでも磁気飽和しないセンサが製作できることが分かった。しかし、透磁率の高いワイヤ（比透磁率17000以上）と比べて、MIセンサでは感度が低くなってしまう。

本研究で開発するIPAセンサでは、感磁部アモルファスワイヤを複数用いて高感度化するため、この問題を克服可能であると考えられる。

E．結論

微細コイルと透磁率調整を行ったアモルファスワイヤを用いることにより、再生医療用の心筋シートの品質評価やポータブル心磁計に適した IPA センサが製造できる。

厚生労働科学研究委託費（医療機器開発推進研究事業）
委託業務成果報告（業務項目）
研究課題：アモルファスメタル応用のポータブル心磁計開発
業務項目：⑦．センサ信号検出・処理システムの製作
担当責任者：加藤 進輔　フジデノロ株式会社　技術開発部　主任

A．研究目的

IPAセンサを精度良く駆動するために高分解能ADコンバータを用いた信号処理回路を用いている。現段階において当研究グループが運用している磁気計測システムの分解能は磁気換算で約500pTであり、生体磁気計測に応用するためには１桁以上の分解能の向上を目指す必要がある。本研究ではセンサエレメントの高感度化と平行して、信号処理回路のノイズを現行の0.15mVから0.01mVに低減することを目指す。ノイズの原因を分析し対策を検討するとともに、来期以降に試作する予定の心磁計測システム用の信号処理回路としてノイズ対策を盛り込んだ回路構成を構想する。

（倫理面への配慮）

本業務項目は試験用評価機器の開発および機器製造方法の開発であり、倫理面への配慮は必要なし。

B．信号処理回路のノイズ原因の分析と対策の検討

1．パルス同期離散サンプリングに伴うエイリアスノイズ

現行の信号処理回路の構成（図⑦-1）を示す。

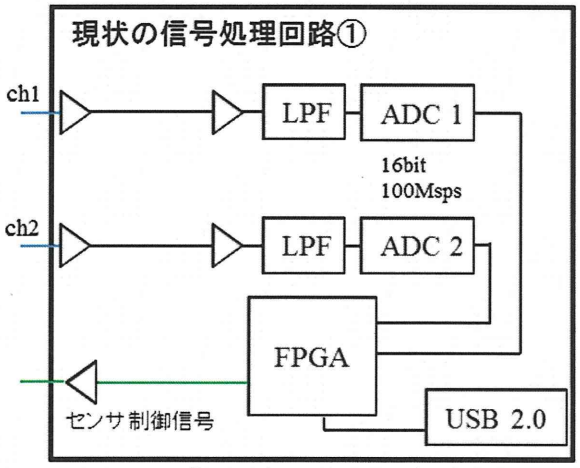


図⑦-1：信号処理回路 1

センサ制御信号に呼応して出力されるIPAセンサの出力電圧（ch1, ch2）を2つの高速16ビットADコンバータを用いて同時に測定する仕様である。100 Mspsで高速に動作するADコンバータによって1回のセンサ制御信号につき磁気信号に比例する電圧データを10～100回程度サンプリングすることができる（図⑦-2）。

このように得られたデータを加算平均して1回のセンサ制御信号についての測定値を1個得るのであるが、データを加算平均する時間範囲が狭いと高周波のノイズ成分がエイリアスノイズとして回路の分解能に影響することが分かった（図⑦-3）。

平均化区間をできる限り広く採り、制御信号周期に近づけることでエイリアスノイズの振幅を低減することができる。

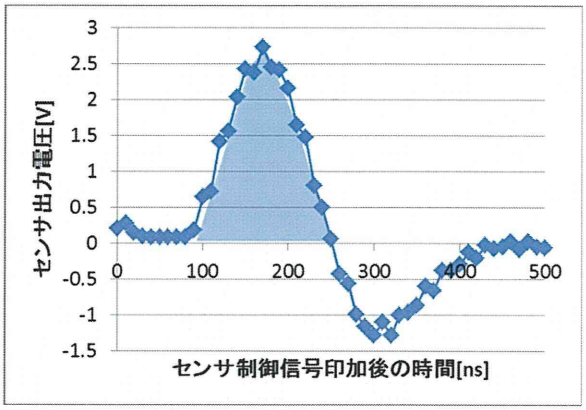


図⑦-2：センサ出力波形

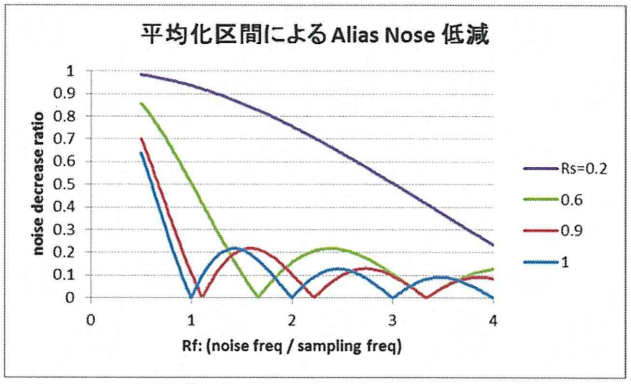


図⑦-3：エイリアスノイズ

②ADコンバータに内在するゲインノイズ

図⑦-1の回路の2つのADコンバータ内部にそれぞれ相関のないノイズ成分がもともと発生しており、差分演算によって除去できないことが性能の限界となっている。そこで信号処理回路を改造し、1つのADコンバータで2つのセンサ出力信号を交互に計測するようにした（図⑦-4）。

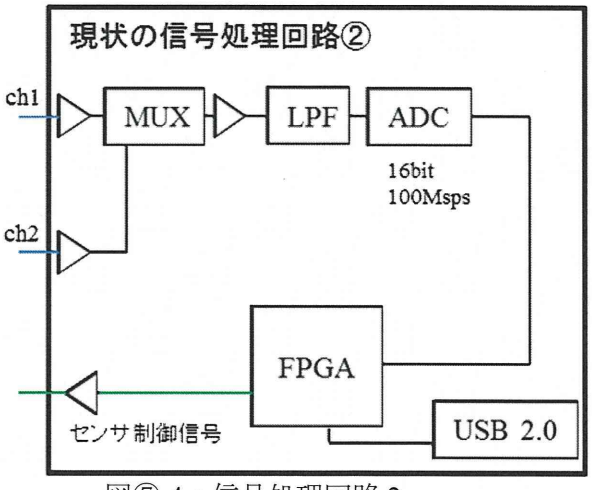


図⑦-4：信号処理回路 2

その結果ADコンバータに起因する低周波のノイズ成分はch1とch2の測定結果の差分処理により大幅に低減することができた。（ノイズRMS値として0.15mVから0.02mVに低減。）また、この回路のch1とch2に異なる大きさの直流電圧信号を入力してノイズの挙動を観察した結果、入力電圧の大きさに比例して、ch1とch2に時間的相関のあるノイズが観察された（図⑦-5）。このことから回路のノイズの主成分はADコンバータに固有のゲイン誤差の時間的な変動であることが判明した。

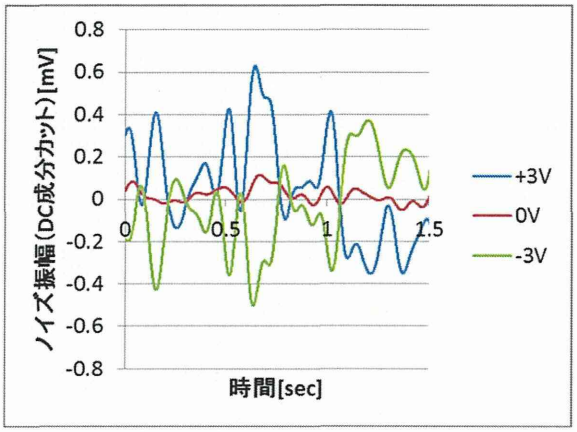


図⑦-5：差分処理後のノイズ

この回路構成においては、環境磁気ノイズとして制御信号周期の2倍の周期をもつノイズがch1とch2に同程度入力された場合、差分処理によって振幅が2倍のエイリアスノイズとなって現れてしまうという致命的な問題があることが分かった。この問題を解決するためには2つのADコンバータによる2ch同時計測は必須であり、その場合にはゲインノイズを低減するために個々のADコンバータのゲイン誤差の変動を高速で補正を行うことが有効であると考えられる。

C．ノイズ低減を狙った信号処理回路の構成検討

以上のようなノイズによる分解能のボトルネックを改善するため、2つのADコンバータを用いた新しい方式の信号処理回路の構成および信号処理方法を検討した（図⑦-6）。この回路は現状よりも2倍高速な200Msps・16ビットADコンバータを2個搭載し、ノイズ対策として以下の機能を採用する。

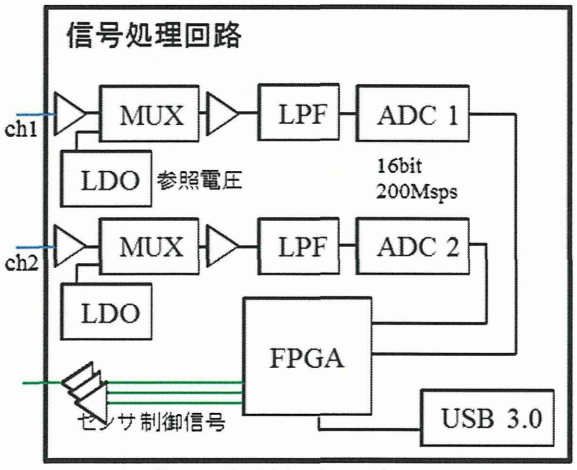


図⑦-6：信号処理回路 3

1. サンプリング頻度の倍増による計測精度向上

現行の100Msps16bitADCでは図⑦-1のようにセンサ出力の変化を捉えるにはデータ点が粗いため、MHz帯の高周波ノイズがエイリアスとして分解能に影響することが無視できない。更に高速な200Msps16bitADCを採用し、オーバーサンプリングによる高周波ノイズの平均化効果を高める。

2. センサ出力の2つの時間領域の時分割計測による信号強度の増加

センサ出力には、センサ制御信号の立ち上がりタイミングに呼応し測定対象磁場に正比例する部分と、センサ制御信号の立ち下りタイミングに呼応し測定対象磁場に逆比例する部分がある（図⑦-7）。現行の信号処理回路では、正比例する部分のみをサンプリングしているが、新たな回路では逆比例する部分もサンプリングし、正比例する部分の平均値と逆比例する部分の平均値をデジタル演算によって差分処理することで、磁気に比例する信号成分の精度をさらに高めることができる。

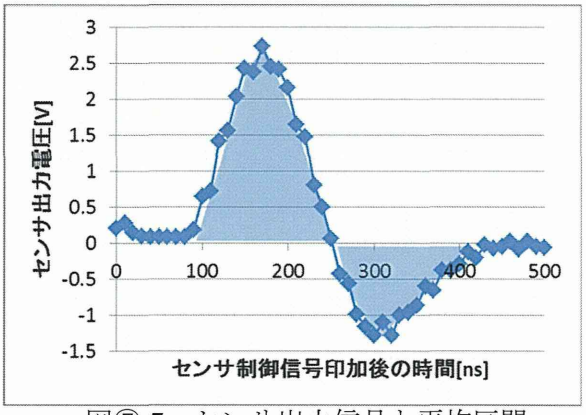


図⑦-7：センサ出力信号と平均区間

3. センサ信号の2つの時間領域の時分割計測によるオフセット誤差除去

図7のように2つの時間領域に分けてデジタル差分処理することは、副次的に低周波ノイズ成分であるオフセット誤差の変動によるノイズを除去する効果も期待できる。このような信号処理をしたときのノイズ除去効果の周波数特性はセンサー制御信号周波数付近を通過域とするバンドパスフィルタ特性を持ち、低周波ノイズおよび高周波ノイズのゲインを1以下に低減することができる（図⑦-8）。

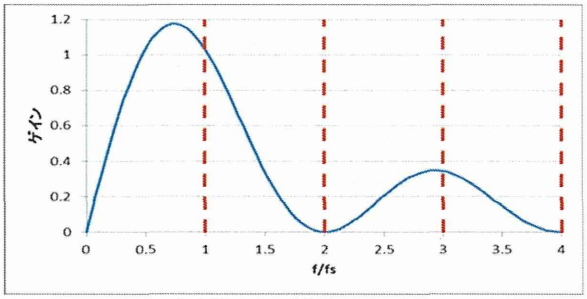


図⑦-8：ゲイン

4. 参照電圧の時分割計測によるゲイン誤差補正

センサ出力信号をサンプリングした直後に、ADッコンバータの入力をマルチプレックス機能を用いて参照電圧に切替える。そのように処理すれば、設計上の参照電圧と実測値との誤差からADコンバータのゲイン誤差を算出し、これを用いてセンサ出力信号の計測値に含まれるゲイン誤差を補正する。このような参照電圧測定によるゲイン誤差補正をセンサ制御信号の周期ごとに高速に行うことで、ゲイン誤差の変動によるゲインノイズを除去することができる。

ノイズの除去と補正に関するデジタル演算は

$$V=(V1-V2)*Vref/V3$$

V1：センサ出力の1つ目の時間領域、
V2：センサ出力の2つ目の時間領域、
V3：参照電圧の時間領域、
Vref：参照電圧の設計値

と表される。

5. センサ制御信号の出力可変機能による励磁条件の最適化

センサ制御信号を出力するアンプを複数並列に配置し、その出力タイミングを段階的にONにしてステップ波形のような緩やかな電流増加によってワイヤを励磁することを検討する。これにより、センサの立ち上がり起電力波形のピーク電圧を立ち下がり波形と同程度まで鈍らせることで、入力レンジに対する信号振幅が上下限いっぱいまで振れるようにゲインを最大化する。

D．考察

以上のようなノイズ対策および測定精度改善の方策を適用した信号処理回路によって、現行の回路に対して分解能を一桁改善することを狙う。それぞれの方策は、現行の回路のノイズの分析により得られたものであり、これらを改善した新たな回路を運用することで、現状は認識できていない新たなノイズ原因の特定と更なる分解能向上の方策についての検討が可能となることが期待される。

E．結論

今年度は、現状のIPAセンサ用信号処理回路について、ノイズの分析と対策の立案を行い、分解能を一桁向上させる新規回路の構成を検討した。次年度においては、それぞれの改善方策について、試作回路を用いた実験実証を行い、必要な性能の確保の目途付けをするとともに、具体的なポータブル心磁計用の信号処理回路の設計に着手する。

様式第１９

# 学　会　等　発　表　実　績

委託業務題目「アモルファスメタル応用のポータブル心磁計開発」
機関名　国立大学法人名古屋大学

１．学会等における口頭・ポスター発表

| 発表した成果（発表題目、口頭・ポスター発表の別） | 発表者氏名 | 発表した場所（学会等名） | 発表した時期 | 国内・外の別 |
|---|---|---|---|---|
| Mechanisms of Biomagnetic Waves in Gut Musculature. ・口頭 | 中山晋介・内山剛 | 第８８回日本薬理学会 | 2015/3/20 | 国内 |
| Biomagnetic Vector Fields of Gut Functional Syncytium. ・ポスター発表 | 中山晋介・内山剛 | 第９２回日本生理学会 | 2015/3/22 | 国内 |
| | | | | |
| | | | | |
| | | | | |

２．学会誌・雑誌等における論文掲載

| 掲載した論文（発表題目） | 発表者氏名 | 発表した場所（学会誌・雑誌等名） | 発表した時期 | 国内・外の別 |
|---|---|---|---|---|
| Real-time measurement of biomagnetic vector fields in functional syncytium using amorphous metal. | 中山晋介・内山剛 | Scientific Reports | 2015/3/6 | 国外 |
| | | | | |
| | | | | |
| | | | | |
| | | | | |

（注１）発表者氏名は、連名による発表の場合には、筆頭者を先頭にして全員を記載すること。
（注２）本様式はexcel形式にて作成し、甲が求める場合は別途電子データを納入すること。

SCIENTIFIC REPORTS

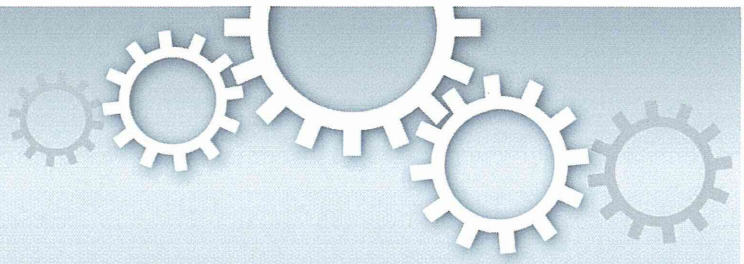

OPEN

SUBJECT AREAS:
SENSORS AND PROBES
BIOMEDICAL ENGINEERING

Received
29 October 2014

Accepted
6 February 2015

Published
6 March 2015

Correspondence and requests for materials should be addressed to S.N. (h44673a@nucc.cc.nagoya-u.ac.jp)

# Real-time Measurement of Biomagnetic Vector Fields in Functional Syncytium Using Amorphous Metal

Shinsuke Nakayama[1] & Tusyoshi Uchiyama[2]

[1]Department of Cell Physiology, Nagoya University Graduate School of Medicine, Nagoya 466-8550, Japan, [2]Department of Electronics, Nagoya University of Graduate School of Engineering, Nagoya 464-8603, Japan.

**Magnetic field detection of biological electric activities would provide a non-invasive and aseptic estimate of the functional state of cellular organization, namely a syncytium constructed with cell-to-cell electric coupling. In this study, we investigated the properties of biomagnetic waves which occur spontaneously in gut musculature as a typical functional syncytium, by applying an amorphous metal-based gradio-magneto sensor operated at ambient temperature without a magnetic shield. The performance of differentiation was improved by using a single amorphous wire with a pair of transducer coils. Biomagnetic waves of up to several nT were recorded ~1 mm below the sample in a real-time manner. Tetraethyl ammonium (TEA) facilitated magnetic waves reflected electric activity in smooth muscle. The direction of magnetic waves altered depending on the relative angle of the muscle layer and magneto sensor, indicating the existence of propagating intercellular currents. The magnitude of magnetic waves rapidly decreased to ~30% by the initial and subsequent 1 mm separations between sample and sensor. The large distance effect was attributed to the feature of bioelectric circuits constructed by two reverse currents separated by a small distance. This study provides a method for detecting characteristic features of biomagnetic fields arising from a syncytial current.**

Many tissues have a cellular organization designed to conduct an electric current, so as to achieve their functions. Nerve impulses are conducted in axonal fibers, conveying cellular information toward target cells. Cardiac pacemaker potentials propagate throughout the atrium and ventricle to produce synchronized heart beats. Other examples of functional syncyti (i.e. many cells electrically coupled to act synchronously) exist throughout the body, especially in the autonomic nervous system. The well-known coordinated motions of gut musculature, such as peristalsis and segmentation[1,2], are one particular instance of cooperative electric activities of the syncytium.

The conduction of an electric current induces a magnetic field. This should hold true for biological systems. Magnetometers to measure biomagnetic fields would thus provide non-invasive and aseptic estimations of how cellular organizations electrically communicate and affect function. Such devices would need to be sensitive to detect small signals from small biological samples, ideally in real time and should not an need elaborate or expensive infrastructure, so that they can be routinely and universally used in laboratory and hospital settings. Current methodologies to detect biomagnetic fields are operated with several requirements. For instance, superconducting quantum interference devices (SQUID) are placed in a liquid coolant container and thus limit their ease of use[3,4]. In the case of atomic magnetometers, significant heating (180–200°C) is normally applied to produce sufficient alkaline metal vapors for the necessary sensitivity[5]. Also, both magnetometers need to be shielded against the geomagnetic field, because of saturation.

In this study, we show quasi-real-time measurements of biomagnetic vector fields in typical functional syncytia of gut musculatures, by using an improved amorphous metal-based magneto sensor, which is operated at ambient temperature without a magnetic shield. We incorporated a gradio-type magneto sensor device constructed with a single magnetic amorphous wire and a pair of transducer coils on both ends. In gut musculature samples isolated from guinea-pigs, magnetic waves up to several nT were stably observed under physiological conditions. The polarity of magnetic waves was altered depending on the relative angle of the muscle layer and magneto sensor, indicating the existence of propagating intercellular currents. We also observed a rapid reduction of the magnitude of biomagnetic fields within a small distance from the tissue. Our practical and computational simulations

demonstrate that this can be attributed to the feature of bioelectric circuits constructed by a propagating intercellular current and extracellular return currents separated by a small distance.

## Results

**Magneto sensor system.** Figure 1 shows a set of diagrams for the magneto sensor system used in this study. The gradio-magneto sensor device (a) is made of ordinary electro-magnetic materials, and is operated at room temperature. Thus, biomagnetic fields that closely approach those of samples can be measured (b). Gradio-magneto sensors require a pair of detectors for both the biological sample and environmental magnetic fields ($M_{b+e}$), and for the environmental magnetic field alone. MS1 and MS2 are detectors for the former and the latter, respectively (a,c). Subtraction of each output removes environmental magnetic noise, including geomagnetism. We have improved the gradio-magneto sensor device by using a continuous single CoFeSiB amorphous (Am) wire with a pair of transducer coils mounted on both ends. Thus, unlike the gradio-magneto sensor device previously made by a pair of magneto-impedance elements[6,7], this device is physically inseparable. Application of an excitation-pulse ($P_e$) (d) induces induction potentials in the transducer coils of MS1 and MS2, which are similar in amplitude and decay time course (e) in the absence of the sample magnetic field. This is ascribed to the symmetrical magnetic field towards both ends of the wire. Also, it is noted that although this sensor uses an analogous device of a magneto-impedance element (i.e. a transducer coil with an amorphous metal wire), it does not measure the impedance of the amorphous wire during application of an AC current, but measures the amplitude of the induction potential in transducer pickup coils upon application of an excitation pulse (For more details see Methods, and Fig. S1).

Figure 2 shows the determination of specifications for the gradio-type magneto sensor with a continuous single amorphous wire. An insulated electric cable (1 mm in diameter; 30 cm in length) is placed at the center of MS1 (a, b), and the amplitude of the current applied to the cable and the gap between MS1 and the cable is changed (c–e). The output potential of the magneto sensor increased in proportion to the electric current amplitude (R = 1.00), indicating a linear voltage conversion of the objective magnetic field. Also, as the gap between MS1 and the cable increased (gap distance), the output decreased inversely (f). From the relationship between the output potential and gap distance, the sensitivity of the magnetic field was estimated to be ~25 μV/nT.

**Biomagnetic field measurement.** Biomagnetic fields were measured in musculatures isolated from guinea-pigs without using any magnetic shield. The sample was fixed in a recording chamber on MS1 (Fig. 3a). Environmental magnetic noise was removed by subtracting the MS2 signal from that of MS1 in this magneto sensor system. Also, during biomagnetic field measurements, the recording chamber and the near-by magneto sensors were kept at 34–36°C, using a plastic panel heater. Panel b (Fig. 3b) shows an example of recording spontaneous magnetic activity in an ileal musculature mounted with the longitudinal muscle layer down and perpendicular to MS1 in the recording chamber. Application of a $K^+$ channel blocker (0.5 mM tetraethyl ammonium: TEA)

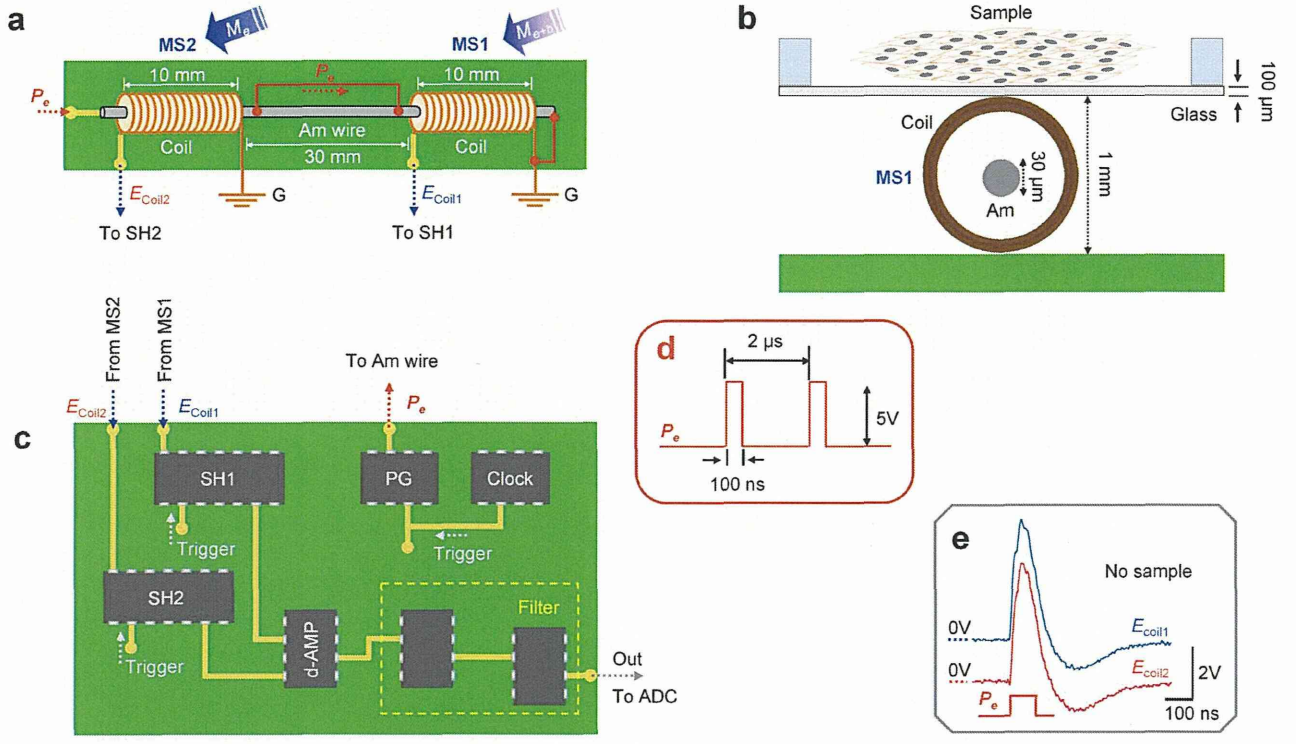


**Figure 1 | Schematic diagram of a gradio-magneto sensor system.** (a) A gradio-magneto sensor device was composed of a single amorphous metal (Am) wire (50 mm in length) with a pair of detector coils (10 mm in length; 300 turns) mounted at both ends. MS1 was placed below a recording chamber, while MS2 was placed ~30 mm apart from MS1 in the same direction. MS1 and MS2 received driving electric pulses ($P_e$). The intermediate part of the wire (30 mm) was electrically shunted. (b) The Am wire was placed in a plastic bobbin (~1 mm diameter) surrounded by a transducer coil. The sample was separated by a cover glass (100 μm thick). (c) A pulse gate IC (PG) triggered by a clock IC. The same clock IC also triggers sample-and-hold detectors (SH1, SH2) to measure the voltage of the transducer coils in MS1 and MS2. A fast operation amplifier (d-AMP) differentiates the voltage in SH2 from that in SH1. Output signals were filtered by high and low-cut filters (H/LPF: 0.5 Hz and 20 Hz) and stored in computer memory via an analog-to-digital converter (ADC). (d) $P_e$ (100 ns, 5 V) applied at 2 μs intervals. (e) Pickup coil potentials in MS1 and MS2 ($E_{coil1}$ and $E_{coil2}$) measured upon application of $P_e$ without a sample.

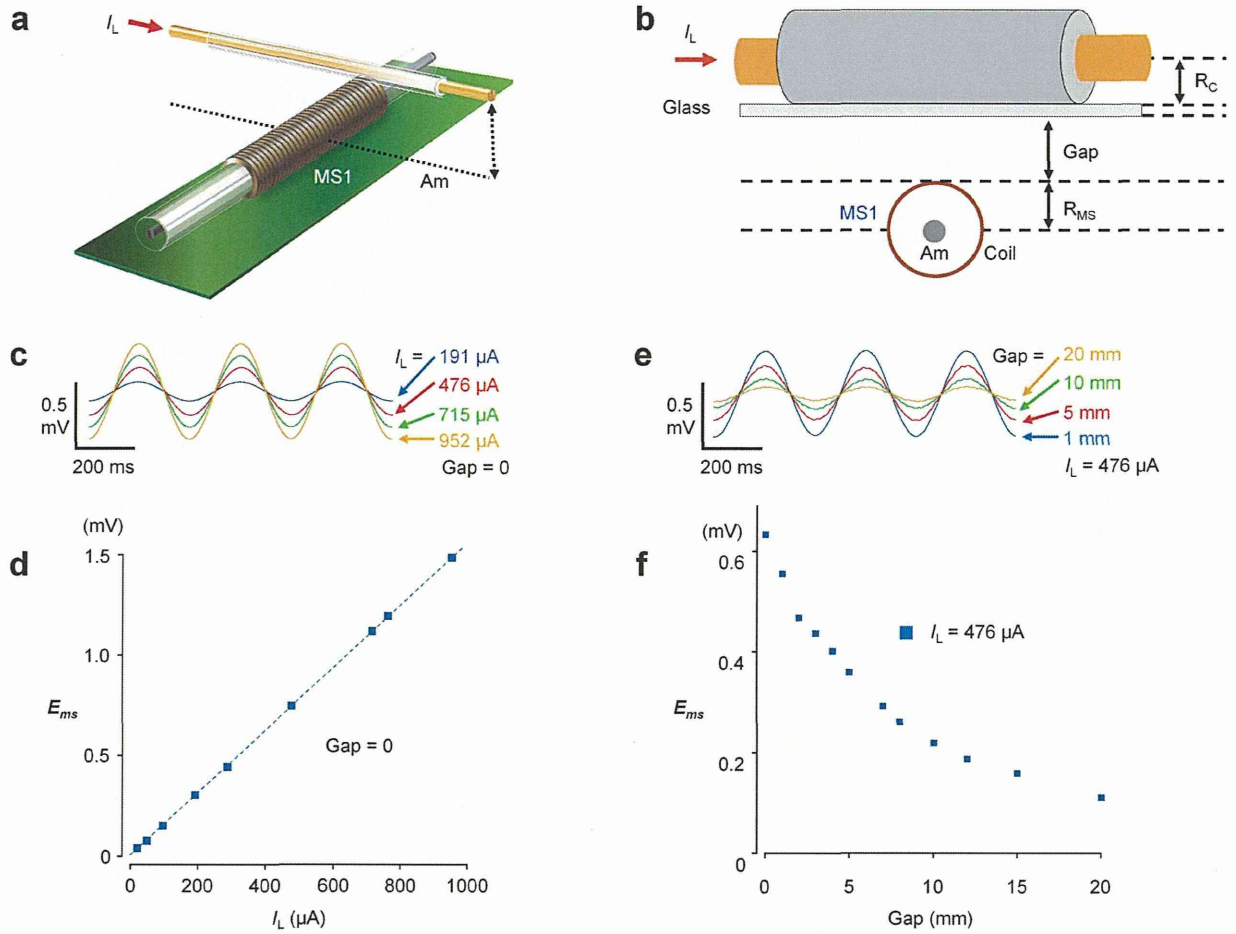


**Figure 2 | Detection efficacy of the improved gradio-magneto sensor system with a continuous Am wire.** (a,b) A linear cable (30 cm in length, 0.5 mm in radius: $R_c$) in which a current generator provides oscillating sine waves of 3 Hz. Various amplitudes of the linear cable current ($I_L$) were applied, and the linear cable was raised with various gaps. (c,d) Changes in the output voltage of the magneto sensor amplifier ($E_{ms}$) by applying various $I_L$ with no gaps. (e,f) Changes in $E_{ms}$ by shifting the $I_L$ gap distance by 476 μA.

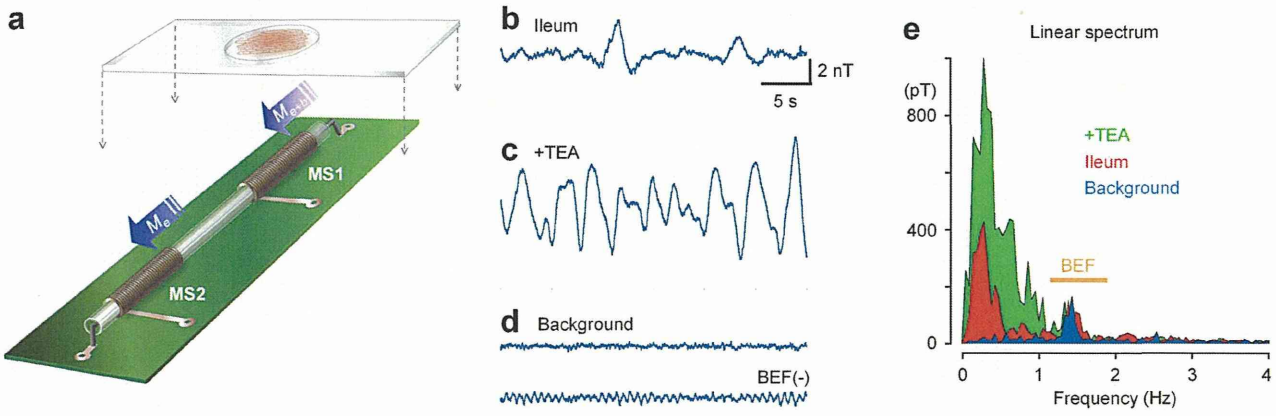


**Figure 3 | Quasi-real-time measurements of biomagnetic fields from an ileal musculature.** (a) The sample was fixed in a recording chamber on MS1. MS1 detects biomagnetic fields along with environmental magnetic fields, while MS2 detects only the latter. Environmental magnetic fields were canceled by subtracting the MS2 signal from MS1 signal. (b) An example of a real-time measurement of biomagnetic activity in an ileal musculature sample in normal solution. The sample was mounted with the longitudinal muscle layer down, and perpendicular to the MS1. (c) Spontanoous biomagnetic activity was applified by application of TEA (0.5 mM). A band elimination filter (BEF) was applied in off-line analysis in (b) and (c). (d) Background noise traces with and without BEF. (E) Linear spectra of b, c and d. The yellow line represents the frequency range of BEF applied in (b–d).

significantly enhanced the magnetic activity (c), in accordance with its excitatory effects on electric activity[8]. The active magnetic fields observed are considered to reflect the ability to propagate electric activity in electric syncytia of the musculature. The gradio-magneto sensor measurements usually contained a low frequency noise of ~1.4 Hz (d, upper trace), but a band elimination filter effectively reduced the background noise (d, lower trace). Linear spectra (e) and histograms (Fig. S2) extracted the amplification features of biomagnetic fields in the presence of TEA, compared with the background noise. Since dihydropyridine $Ca^{2+}$ channel antagonists nearly completely abolished the response to TEA (Fig. S3), it was suggested that the enhancement of magnetic activity employed electric currents in smooth muscle cells.

**Distance and direction of the sample.** The magnitude of a magnetic field is reduced depending on the distance between the sensor and electric current source. We thus examined the effects of gap distance between the sample musculature and MS1, as shown in Fig. 4a. As the gap distance increased to 1 and 2 mm, the biomagnetic waves of ileal musculatures decreased rapidly, as seen in magnetic field traces (b–d) and in linear spectra (e–g) measured in the presence of TEA. Changes in the biomagnetic field were quantified by integrating a linear spectrum in the range of <1.2 Hz, avoiding low frequency noise. The magnitude of the biomagnetic field decreased to 30.3 ± 8.2% (n = 10) and to 10.5 ± 2.4% (n = 4) when the gap distance was 1 and 2 mm, respectively, in normal solution (h), and it decreased to 37.9 ± 12.0% (n = 6) and 16.6 ± 5.0% (n = 6), when the gap distance was 1 and 2 mm, respectively, in the presence of TEA (i).

The direction of magnetic field changes depended on the propagating direction of the electric current. Thus we assessed the effect of reversing the direction of the musculature sample on MS1 (the rotation of the sample and MS1) on the signal output (Fig. 4j–m). In j, an ileal musculature crossed MS1 from the anal-to-oral ends, observed from the bottom side of the sensor. The magneto sensor recorded many magnetic waves consisting of an upstroke component (red arrow head) followed by a downstroke component. Subsequently, the direction of the ileal musculature was reversed, crossing MS1 from the oral-to-anal ends, as shown in k. This procedure reversed the direction of magnetic waves. Four large magnetic waves in j and k are shown expanded in l and m, respectively, clearly indicating the reverse of biomagnetic fields. Since positive (upward) signals in the sensor output represent the rightward direction of the magnetic field (MS2 is placed to the left of MS1; positive signals represent the direction of MS2 to MS1), the magnetic waves in Fig. 4j–m correspond to a propagating electric current in the oral-to-anal direction in this sample.

The effect of reversing the musculature direction was also examined in stomach samples, because the propagation direction of electric activity appears to persist for a long time[8]: Each reversed direction of the musculature sample changed the direction of the magnetic field (Fig. S4). Essentially similar results were obtained in other ileal (n = 5) and gastric musculature (n = 4) samples. These results reinforce that gradio-magneto sensors can detect magnetic fields of a propagating electric current in the syncytia of musculatures, but are not significantly influenced by musculature vibrations[9], which may affect the susceptibility of amorphous metal wires through magnetostrictive effects.

**Simulations of biomagnetic fields.** The biomagnetic field decreased rather rapidly as gap distance increased (Fig. 4h,i), compared with the magnetic field measurements with a single electric cable. To account for this, we assumed that the electric current propagated in the musculature sample was accompanied by a return current, with an effective distance between these currents of several hundred μm. Figure 5 shows magnetic field measurements from a practical model in which two electric cables (1 mm diameter; 30 cm in length) are piled one upon the other separated by a thin glass (100 μm) (a,b). The output of the magneto sensor also increased in proportion to the electric current amplitude applied (R = 1.00), but the gradient was significantly smaller than that examined in a single electric cable (3.2 *vs* 15.5 V/A) (c,d). Also, the gap distance decreased the signal output in two parallel cables more effectively than in a single cable. The amplitude was reduced to ~27% at 5 mm.

Due to the limitations of a lab-made practical model in which the length of electric current segments vertical to the sensor are significantly longer than those of in parallel (see more detailed explanation in the Appendix in SI), we next assessed the distribution of the biomagnetic field using computer models (Fig. 6). We assumed the propagating intercellular current and return extracellular current distribution by simplifying with five combined rectangular circuits (a,b). The pseudo color maps display that the magnetic field decreases rapidly as the distance from the rectangular circuit increases; for example, it decreased to ~30% between 1 and 2 mm from the circuit. The magnetic field was amplified by increasing the loop distance (c). As shown in the practical and computer models (Figs. 5 and 6; Figs S5–S7), the rapid reduction of biomagnetic fields with a small distance can be attributed to the features of biological electric circuits constructed by intercellular and transmembrane ionic conductions. Namely, a major propagating intercellular current and return extracellular currents are separated by a small distance, at least less than the thickness of samples. In other words, the size of an effective circuit for generating a biomagnetic field is rather small, presumably in the range of several hundreds of μm to several tens of mm (within the size of electric syncytium at most).

## Discussion

The musculature of the gastrointestinal tract is known to act as a group of electric syncytia to achieve its function. When a part of the syncytium receives chemical or electric stimuli, electric signals propagate through intercellular electric connections, i.e. gap channels, organizing the syncytium and allowing it to respond as a whole. Electric connectivity of gut musculatures has been shown by conventional microelectrodes[10] and a microelectrode array (MEA)[8]. However, the experiments with microelectrodes were carried out using an electric current injector, while the MEA measurements merely showed spatial synchronizations of electric activity.

In the present study, we detected biomagnetic fields in gut musculatures, using an amorphous metal-based magneto sensor in a quasi-real-time manner (Fig. 3). The measurements demonstrated a vector feature of biomagnetic fields reflecting the propagation direction of spontaneous electric activity (Fig. 4 and Fig. S4). In addition, the amplitude of magnetic waves represents the conductivity of electric activity. These parameters provide us with new functional information of cellular organizations. Furthermore, we observed a rapid reduction of the magnitude of magnetic activity by increasing the distance between the sensor and sample (Fig. 4): ~30% decreases by the initial and subsequent 1 mm separations. Along with the practical and computer simulations of biomagnetic fields (Figs. 5 and 6), this observation can be attributed to a rather small size (<1 mm thick) of effective electric circuits in the cellular organizations examined in the present study. This feature of a bioelectric circuit can also account for the limitations of measurements in small biological samples using a SQUID whose detector coils are placed in a liquid container[11]. In line with this deduction, previous volume conductor models for an isolated whole heart, have displayed a slower reduction of magnetic fields (from 1 nT to 100 pT with a separation of ~10 mm)[12].

Under control conditions, the amplitude of magnetic waves measured in ileal musculatures was within the range of several nT, when the MS1 sensor was placed below the recording chamber (Fig. 3). Since MS1 detectors and samples are separated by a cover glass of ~100 μm, and the amorphous wire of MS1 (=MS2) is surrounded by a transducer coil with a 500 μm radius, the total distance between

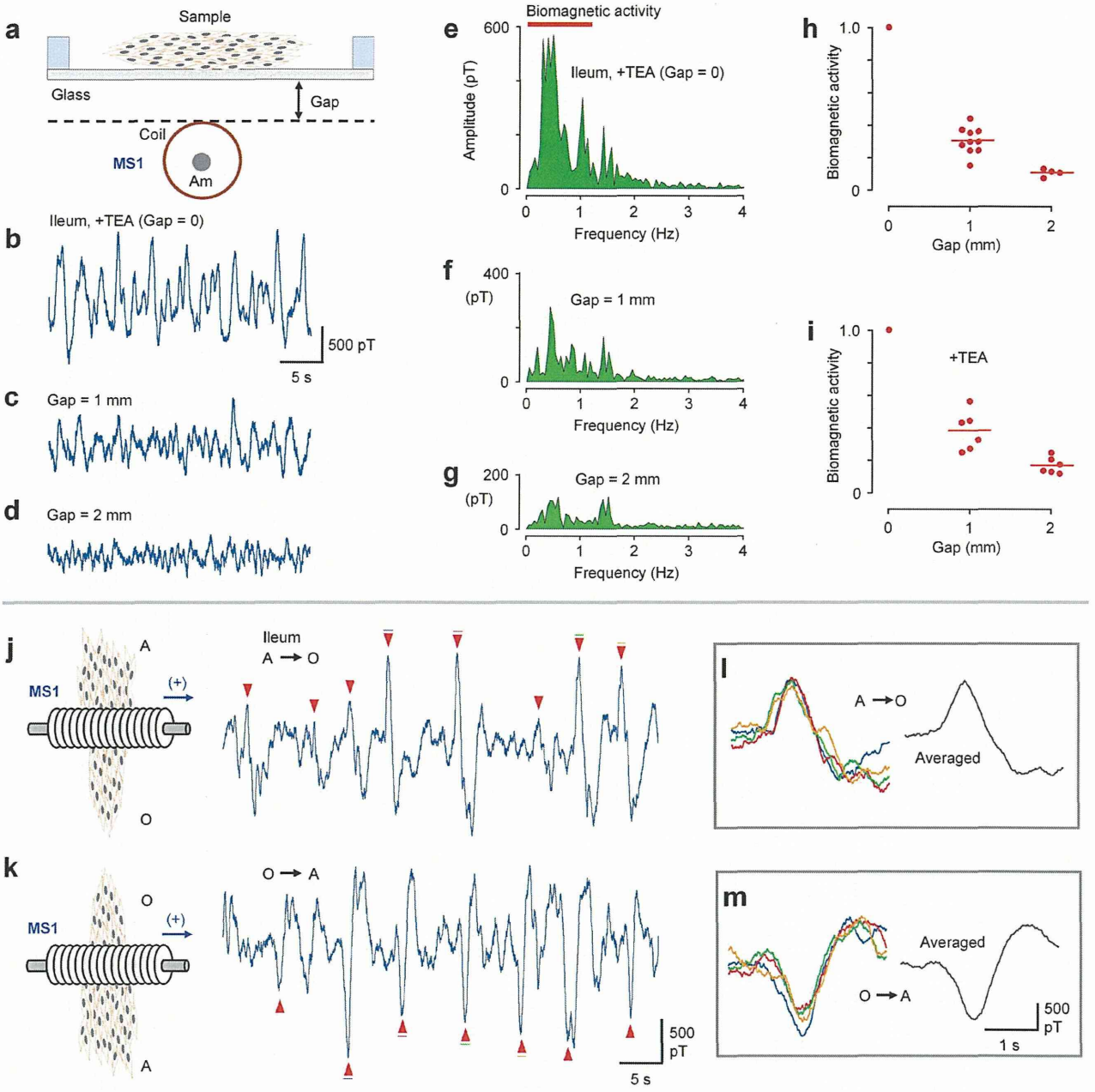


**Figure 4 | Biomagnetic fields characterized by gap distance (a–i) and direction of musculature (j–m).** (a–d) Gap distance between the cover glass and MS1 magneto sensor was changed from 0 to 1 and 2 mm, in the presence of a $K^+$ channel blocker (0.5 mM TEA). (e–g) Linear spectra for the magnetic field recordings B to D. Note that increases in gap distance largely reduced the signals < ~1.2 Hz, while the magneto sensor noise remains at around 1.5 Hz. (h,i) Sum of linear spectrum amplitude in the frequency range indicated in (e) (thick red line) is plotted as biomagnetic activity against gap distance, relative to that without a gap, in the absence and presence of TEA. Thin red lines represent the average of experiments. (j,k) Biomagnetic field measurements from the same ileal musculature that crossed the MS1 magneto sensor in anal-to-oral (A → O) and oral-to-anal (O → A) ends, respectively. Gap = 0. The schema indicates the bottom view of the sample and magneto sensor. (l,m) Four expanded biomagnetic waves in (j) and (k) are superimposed (left) and averaged (right) in (l) and (m), respectively. Biomagnetic waves used are indicated by color bars in (j) and (k).

the magneto sensor (the center of the amorphous wire) and the propagating major intercellular current is assumed to be ~1 mm. On the other hand, the computer models with a distance of 0.2–0.5 mm between intercellular currents and return currents (Fig. 6 c, left and center maps) better reflect ileal musculatures. In the maps of these models, the total circuit current was 5 μA, and the magnetic field at 1 mm below the intercellular current is estimated to be ~200–300 pT. Also, previous sucrose-gap voltage-clamp experiments and theoretical analysis indicate that a small length (0.5 mm) of gut musculature requires a transmembrane electric current of more than several to several tens of μA at depolarizations corresponding to spike activities[13,14]. Therefore, the magnitude of biomagnetic fields observed in this study (up to several nT) may correspond to electric activities of only a part of musculature samples (25 mm long × 5 mm wide). In future studies, we may need to consider this issue (the ratio of active region) by using a magneto